Active Control of Tool Position in the Presence of Nonlinear Cutting Forces in Orthogonal Cutting

A.H. El-Sinawi
Mechanical Engineering department
American University of Sharjah,
Sharjah, UAE PO Box 26666

aelsinawi@aus.edu

Abstract

This work presents a practical approach to the control of tool's position, in orthogonal cutting, in the presence nonlinear dynamic cutting forces. The controller is Linear Quadratic Gaussian (LQG) type constructed from an augmented model of both, tool-actuator dynamics, and a nonlinear dynamic model relating tool displacement to cutting forces. The latter model is obtained using black-box system identification of experimental orthogonal cutting data in which tool displacement is the input and cutting force is the output. The controller is evaluated and its performance is demonstrated.

Key words: LQG, Nonlinear ARX Model, Orthogonal Cutting, Active Control, Nonlinear Cutting Force

1. INTRODUCTION

Performance of machining processes is assessed by dimensional and geometrical accuracy as well as the surface texture of the part. Factors such as cutting force, workpiece vibration, machine-tool vibration, process instability, tool wear and thermal deformation deteriorate this performance. Recent interest in high speed-machining and high manufacturing efficiency requires faster, higher bandwidth actuation, and controllers that are more robust. Besides determining part functional behavior, the surface texture also plays a key role in the area of manufacturing process control [1]. The basis for using surface texture as means of process control is derived from the fact that a slight change in the manufacturing process manifests itself as a corresponding change in the resulting surface geometry. The roughness, waviness, lay, and flaws constitute the texture of the workpiece surface [2]. Surface texture of the work-piece is highly dependent on tool position during cutting which in turn is affected by cutting dynamics. Therefore extensive research work has been done on modeling and analysis of tool work-piece interaction and the dynamics of the cutting process. Altintas [3] have presented a cutting force model as a function of regenerative chip thickness, cutting speed, and the velocity and acceleration terms of the vibrations. In their work, amplitude and frequency of inner and outer vibration waves are generated on the chip by an instrumented fast tool servo powered by a piezo actuator. They established a model in which the coefficients of dynamic cutting forces are identified and used in analyzing the effect of cutting speed, tool wear, vibration frequency and wavelength on the chatter stability of a turning process. Ikua [4] have studied the cutting force generated in ball end milling and presented a model for the radial and tangential forces as a function of depth of cut, and other factors related to the geometry of the tool and workpeices.

Researchers have tried to establish quantitative relations between the surface finish and the cutting parameters of the depth of cut, feed, and cutting speed using methods such as, among others, wavelength decomposition surface roughness, wavelet analysis, and tool vibration [4-9]. The cutter–workpiece interaction forces are assumed to cause relative displacement between the cutter and the work piece, which influence the surface generation mechanism. Analytical, experimental and mechanistic methods were used to predict the interaction forces. The analytical methods focused on establishing a relationship between the cutting force and the instantaneous uncut chip cross – section [10, 11] and the non – linear mechanisms [12, 13]. The analytical models were not capable of predicting the dynamic forces accurately due to the secondary non –

linear effects that stems from the tool/workpiece interaction. The experimental methods include static, dynamic and time–series methods. The static methods are assumed based on linear assumptions and linear cutting conditions [14]. The dynamic methods replaced the static methods and the cutting process is assumed to be a combination of two independent actions namely, the wave cutting action and the wave removing action [15]. The time-series method was formulated to identify the dynamic cutting force coefficients as well as the transfer functions of the three dimensional dynamic cutting process directly from operating data [16]. The mechanistic modeling methods view the machining process as a combination of the chip load/cutting force relationship, cutting – tool geometry, machining conditions and tool /work – piece displacement due to cutting forces. The workpiece dynamic behavior is constructed using either the distributed – parameter [17], or the lumped – parameter approaches [18]. Few researchers investigated the dynamic effect of the tool holder. Shawky and Elbestawi [19] concluded that the effect of tangential force is insignificant and no model of the tool holder is needed in that direction. Their experimental work showed that modeling the tool by a second order system in each axis provides significant approximation of the dynamic behavior of a single point tool during cutting [19].

Control of machining process includes three levels of control that one might encounter in a controller for machining process, namely they are the servo control, the process control [20] and the supervisory control [21]. In the servo control process, the motion of the cutting tool is taken relative to that of the workpiece. The process control level is used to control the cutting forces and tool wear to maintain high production rates and good part quality. The highest level of control is the supervisory control and it directly measures product related variables, such as part dimensions and surface finish. Different approaches are used to correct for machining errors by means of dynamic error compensation. More recently, Tian et al. [22] have presented a methodology for modeling and control of a high precision flexure-based mechanism for ultra-precision turning operation based on the position control of an auxiliary precision mechanism utilized on the turret of the conventional lathe to implement nanometer level infeed. El-Sinawi [23] has presented an optimal control method for controlling the tool position in orthogonal cutting in both feed are radial directions. Moradi et al. , [24] have presented a robust control method for Orthogonal turning process in the process was modeled as a single degree of freedom model that includes the effect of tool flank wear with a control input of the system being force applied to the tool provided by a piezo-actuator. Huang et al. [25] have presented a tool wear detection based on cutting force monitoring.

In this work, a control scheme for the purpose of improving surface texture of turned surfaces through control of tool position in the presence of nonlinear cutting force is developed.

Improvement of surface quality is achieved via active positioning of the tool or cutter through the attenuation of cutting forces effect on the tool in both radial and tangential directions. The process is assumed to be stochastic due to both process and measurement noise. Experimental force-displacement data is used to construct a nonlinear dynamic model of dynamic cutting forces. Various nonlinear models are constructed using system identification techniques including ARX, nonlinear ARX, and Hammerstein-Wiener techniques [26]. The best nonlinear model obtained that closely fits experimental data, is then linearized and constructed in state-space form to later utilize in the Linear Quadratic Gaussian Controller. Simulation results will be used to verify the effectiveness of the proposed modeling and control approach, and to enhance current understanding of the mechanisms responsible for generating both stochastic and deterministic components of the surface texture. Simulation work of the proposed modeling and control techniques will be based on actual parameters for actuators and the cutting process data, which is readily available in the literature [27].

2. MODEL DEVELOPMENT

Force-displacement data obtained from experimental cutting of a 6061 Aluminum workpiece using a carbide tool with $0°$ rake angle and $7°$ clearance angle, depth of cut of 0.4 mm, feed of 0.050 mm/rev, and spindle speed: 2200 rev/min, are shown in Figures 1 and 2, have been used to construct a force displacement model using black-box system identification.

Four dynamic models with tool displacement as input and cutting force as output are constructed are indentified and compared as shown in Figure 3. In reference to Figure 3, the first model identified as LinMod1, is a linear ARX model of the form

$$f_c(t) + a_1 f_c(t-1) + a_2 f_c(t-2) + \ldots + a_\tau f_c(t-\tau) = b_1 x_c(t) + b_2 x_c(t-1) + \ldots + b_\mu x_c(t-\mu-1) + e(t) \qquad (1)$$

Where f_c, x_c are the cutting force and tool displacement in the corresponding direction, respectively. $f_c(t-1) + f_c(t-2), \ldots, f_c(t-\tau)$, $x_c(t) + x_c(t-1), \ldots, x_c(t-\mu-1)$ are delayed input and output variables called regressors. Linear ARX model predicts the output f_c as a weighted sum of its regressors. τ is the number of past output terms while μ is the number of past input terms used to predict the current output f_c and $e(t)$ is a white noise sequence.

The second and third models identified as LinMod3 and LinMod4 are constructed as follows;

LinMod3 is constructed using Predictive Error Minimization or PEM with various constraints on the order or number of states of the state-space model. This method yields a discrete time-domain state-space dynamic model of the form,

$$x(t + Ts) = Ax(t) + Bu(t) + Ke(t), \quad y(t) = Cx(t) + Du(t) + e(t) \qquad (2)$$

In which x are the states, y is output, A, B, C, K, D represent dynamics, input output, disturbance and feed through matrices, respectively [28].

Narx1 model is constructed using Nonlinear ARX model which is an extension of ARX model given in Equation (1) except that the input –output mapping is nonlinear and of the form;

$$f_n(t) = F(f_c(t-1), f_c(t-2), \ldots, x_c(t), x_c(t-1), \ldots) \qquad (3)$$

Where f_n is the output and F is a nonlinear mapping function, such as Wavelet network, Tree partition, etc…, [29].

Nhw1 model shown in Figure 3, is constructed using Hammerstein-Wiener model; see [Yucai Zhu, 2002 and Lennart Ljung, 1999] for further details. It is clear from Figure 3 that the Narx1 has the best fit to experimental data with 99.9% fit.

2.1 Linearization of the Nonlinear ARX Model
The nonlinear model that best fits input-output data is clearly the nonlinear ARX model mapped with a single-layer sigmoid function. The nonlinear mapping of input-output data is shown in Figure 4, with

$$F(v) = L(v - r) + d + g(Q(v - r)) \qquad (4)$$

v is a vector of the regressors. $L(v - r) + d$ is the output of the linear block shown in Figure 4, d is a scalar offset, $g(Q(v - r))$ is the output of the nonlinear function block, and Q is a projection matrix and r is the mean of regressors (v). Function $g(v)$ expressed as $g(v) = \sum_{k=1}^{n} \alpha_k \phi(\beta_k (v - \xi_k))$ with $\phi(s) = (e^s + 1)^{-1}$ is the nonlinearity estimator of the sigmoid function type. β_k is a row vector such that $\beta_k(v - \xi_k)$ is a scalar, s is the Laplace variable and n is the number of sigmoid network units. The model obtained by this approach is of the form given in Equation 3 with $\tau = 4$, and $\mu = 4$.

Step response of the models obtained for both forces in the radial (f_x) and tangential (f_y) directions is shown in Figures 5 and 6, respectively. The step response shows the steady state

values of both functions which are later on used in linearzing the model. See Appendix A for linearization details.

Linearized state-space model of the radial force is;

$$\dot{X}_r(t) = A_r X_r(t) + B_r x_{cr}$$
$$f_x = C_r X_r(t) + D_r x_{cr}$$

(5)

Where $\dot{X}_r(t)$ are the states of the radial force model, A_r, B_r, C_r, D_r are dynamic, input, output and feed through matrices, respectively. f_x, x_{cr} are radial cutting force and radial tool displacement, respectively. The same procedure is carried out for the tangential cutting force model which yields;

$$\dot{X}_t(t) = A_t X_t(t) + B_t x_{ct}$$
$$f_y = C_t X_t(t) + D_t x_{ct}$$

(6)

2.2 Modeling of the Machining Process

Figure7 shows the difference between tool post (passive) and proposed active tool fixture that will allow for implementation of the proposed controller. Figure (7.a) shows the conventional tool post rigidly attached to the machine tool structure, while Figure (7.b) shows the active tool holder platform equipped with two actuators placed between the tool and the machine tool structure. This will allow the control force to provide necessary manipulation of the tool to maintain a constant depth of cut.

During cutting, the tool is perturbed form nominal depth of cut by two inputs namely; the dynamic cutting forces in both radial and tangential directions, in addition to process noise $w(t)$.

State-space model of the tool-actuator assembly in the radial direction can be represented as;

$$\dot{x}_r = A_{cr} x_r + B_{cr} F_{ar}$$
$$Y_{cr} = C_{cr} x_r + D_{cr} F_{ar}$$

(7)

Such that,

$$A_{cr} = \begin{bmatrix} 0 & 1 \\ -\dfrac{k_{ac}}{m} & -\dfrac{b_{ac}}{m} \end{bmatrix}, B_{cr} = \begin{bmatrix} 0 \\ \dfrac{1}{m} \end{bmatrix}, C_{cr} = \begin{bmatrix} 1 & 0 \end{bmatrix}, D_{cr} = 0,$$

where x_r is vector of the tool states, namely, displacement and velocity. m is the mass of the tool and its mount, k_{ac}, b_{ac} are the elastic stiffness and damping coefficients of the actuator, respectively. k_{ac}, b_{ac} can be obtained by an FR test of the tool-actuator assembly. Notice that, the same procedure can be carried out for the tangential direction since both actuators are orthogonal.

Refer to [23, 27] for more information on the model development.

3. CONTROL STRATEGY AND THE CONTROLLER DESIGN

The control strategy will be centered on reducing the amplitude of the tool' dynamic displacement to zero for the purpose of maintaining a constant depth of cut and subsequently, a smooth surface texture of the workpiece. This requires minimization of the error between the desired and the actual position of the tool. The desired or nominal tool position is the one yielding a constant depth of cut. However, the existence of the dynamic cutting forces perturbs the tool form its

nominal position and thus, varies the depth of cut causing subsequent deterioration in surface texture. Attenuating the effect of the cutting force on the tool's position, the error in the tool position will be minimized. This can be achieved by reacting on the tool with an equal but opposite forces through proper actuation. This task is difficult due to (a) existence of process and measurement noise and (b) nonlinearity of the dynamic cutting forces. To overcome these difficulties, the controller must be able to estimate the force needed to minimize the error in the tool position from noisy process using measurement data contaminated with noise. In addition to that, the controller has to track and manipulate the position of the tool effectively in the presence of nonlinear dynamic cutting forces. Added to all of the above, the controller has to maintain high stability and performance under various disturbance characteristics. To do so, the controller has to be constructed based on a model that takes into account the dynamics of the tool-actuator system as well as the cutting force dynamics. Therefore, The plant used for this purpose is a combination (i.e., augmentation) of the dynamic cutting forces and tool-actuator dynamics in both radial and tangential directions. The first step in designing the proposed active controller, is the design of the LQG estimator and regulator gains L_e and K_R, respectively. The analysis presented here is in state-space such that the augmented system depicted by Equations (5), and (6) is;

$$A_a = \begin{bmatrix} A_{cr} & 0 \\ B_r C_{cr} & A_r \end{bmatrix} \tag{8}$$

$$B_a = \begin{bmatrix} B_{cr} \\ B_r D_{cr} \end{bmatrix} \tag{9}$$

$$C_a = \begin{bmatrix} D_r C_{cr} & C_r \end{bmatrix} \tag{10}$$

$$D_a = \begin{bmatrix} D_r D_{cr} \end{bmatrix} \tag{11}$$

where the matrices A_a, B_a, C_a, and D_a are respectively, the dynamic, input, output, and direct transmission matrices of the augmented system. The four matrices in the foregoing are used to design the LQG estimator and regulator gain matrices L_e and K_R, such that,

$$L_e = \begin{bmatrix} [L_{e\,cr}] \\ [L_{e\,r}] \end{bmatrix}, \; K_R = \begin{bmatrix} [K_{R\,cr}] \\ [K_{R\,r}] \end{bmatrix} \tag{12}$$

This augmentation is necessary to incorporate the cutting force dynamics in the process of determining the optimal estimator and regulator gains. Equation 12 shows that L_e and K_R are both partitioned in two parts each where $[]_{cr}$ corrects x_{cr} (i.e., tool-actuator model states) and $[]_r$ corrects X_r (i.e., cutting force states). The LQG (virtual model of the system) should be subjected to all inputs that the actual plant is subjected to, including the control force. Figure 8 shows the control scheme implementation in the radial direction. Further details on construction of the controller are found in [30].

4. NUMERICAL EXAMPLE

Force-displacement results obtained from experimental cutting of a 6061 Aluminum workpiece using a carbide tool with $0°$ rake angle and $7°$ clearance angle, depth of cut of 0.4 mm, feed of 0.050 mm/rev, and spindle speed: 2200 rev/min, shown in Figures 1 and 2, are used to construct a force-displacement model using black-box system identification. Linearized State-space model obtained by Nonlinear ARX modeling, presented here in canonical form is;

$$\dot{X}_r(t) = \begin{bmatrix} 1.145 & -0.7 & 0.5651 & -0.4435 \\ 2 & 0 & 0 & 0 \\ 0 & 1 & 0 & 0 \\ 0 & 0 & 0.5 & 0 \end{bmatrix} X_r(t) + \begin{bmatrix} 1024 \\ 0 \\ 0 \\ 0 \end{bmatrix} x_{cr}$$

$$f_x = 1500 \times [-266.2 \quad 153.9 \quad -213.8 \quad 460.7] X_r(t) + [0] x_{cr}$$

ETREMA actuator with peak-to-peak excursion of $50 \times 10^{-6}\,m$ is utilized as the active manipulator of the tool. The Actuator's elastic stiffness and damping used in this study were taken as follows (El-Sinawi et al. 2005): *m* =0.53 *kg* for the tool-actuator assembly. $k_{ac} = 14.6 \times 10^6$ N/m, and $b_{ac} = 10$ kg /s. The cutting process noise $w(t)$ is assumed to have a zero mean, and variation of $\pm$ 10% of the cutting force, while measurement noise $v(t)$ is also assumed to be random with zero mean, and variation of $\pm$ 10% of measurement values. Notice that the small values of $w(t)$ and $v(t)$ makes the linearization valid in the vicinity of nominal trajectory of the system.

5. RESULTS AND ANALYSIS

To implement the proposed control strategy, experimental force-displacement data shown in Figures 1 and 2 is utilized to construct a transfer function relating the tool's displacement as input to cutting force as output. The data is obtained from Altintas [3] and Matlab® System identification toolbox is used for the purpose of identifying the best transfer function that relates the input to the output. Figure 3 shows various algorithms implemented by the system identification process along with the percentage of match to the experimental input-output data. The figure shows that a transfer function obtained using Narx identification algorithm has a 99.99% match to experimental data. The model obtained from System identification data have the structure shown in Figure 4. Similar approach is used to obtain a transfer function for the input-output data in the feed direction. Step responses of radial and feed transfer function models obtained by System identification are shown in Figures 5 and 6. Latter figures show that both models are lightly damped with damping of approximately 0.5 % and 1 % for the radial and feed directions, respectively. Such light damping should not pose a problem since the damping can be increased using proper feedback control. With the tool's Displacement-Force model in both radial and feed directions are available, the tool is mounted on two orthogonal actuators intended to manipulate the tool's position in corresponding directions using proper control force as estimated by the controller. Transfer functions of the Identified models are augmented with the actuators models to obtain the suitable LQG controller gains Namely, L_e and K_R. During actual implementation of the controller, measurements of the tool position are compared to the estimates of the tool's position and the difference (i.e. error) is fed back through the estimator gain (L_e) to adjust the controller model and thus, improve estimates of the tool's position. The estimated position is then fed through the actuator's transfer function to produce the negative actuation force needed to maintain a constant depth of cut (i.e., zero tool displacement). The negative force provided by the actuator is only estimate of the external cutting force that perturbs the tool from its nominal position. Force estimates depend mainly on the values weighting matrices Q and R needed to minimize the performance index (J) of the LQG [31]. In general, choosing a larger value of Q compared to R implies the demand for high controller performance. On the Other hand, larger value of R implies minimal control energy. In this work, the process model obtained by the system identification is fairly accurate which allows for large Q. However, the limitation on the actuator force (approximately 500 N) and excursion (50 micrometer) poses a limit on the values of Q and R. In such application, the important factor that determines the performance vs. control energy is main the ratio of Q/R rather than the individual values of each.

In this application the ratio chosen for Q/R is 2. Assuming only 10% process and measurement noise, Figures 9 and 10 show that the proposed control technique has managed to reduce the tools dynamic displacement by approximately 40%. These results are reasonable only if the cutting process remains stable (i.e., no occurrence of chatter) and all factors that are not considered in the model remain unchanged; such factors include tool wear, temperature, micro-hardness variation of the workpiece and workpiece dynamics. Figures 11 and 12 show the control force exerted by the actuator on the tool is well within the capability of the actuator. It should be noted that the identified model will be affected by changes of depth of cut, cutting speed feed-rate and tool wear. Adaptive implementation of the proposed process is possible where the displacement-force transfer function identification is continuously updated as the cutting process progresses. However, the accuracy of the identified model can be a serious drawback of the control technique proposed by this work.

6. CONCLUSIONS

In this research work, active control of an orthogonal cutting process is presented. Nonlinear dynamic cutting force model is generated from actual machining data obtained in both radial and tangential directions. An LQG based controller is developed based on an augmented model of both tool-actuator dynamics and a linearized model of the dynamic cutting force. The control objective is to eliminate the tool's dynamic displacement and maintain a constant depth of cut. Simulation results have shown that the proposed control strategy has managed to significantly reduce the dynamic displacement of the tool with minimal force and calculations efforts even in the presence of significant randomness in the process and measurement as well as the nonlinearity of the cutting force. Experimental study is undergoing to verify the integrity of the controller in real time applications.

ACKNOWLEDGEMENT

7. REFERENCES

[1]. M. Shiraishi and H. Sumiya. "Improvement of Geometrical Errors by Surface Roughness and Tool Position Control". *The Annual Meeting of the ASME*, PED-vol. 45:9-22, 1990.

[2]. M. Sander. *A Practical Guide to the Assessment of Surface texture*. Mahr Perthen, Gottingen, Germany, 1991.

[3]. Y. Altintas, M. Eynian, H. Onozuka. "Identification of dynamic cutting force coefficients and chatter stability with process damping". *CIRP Annals - Manufacturing Technology*, 2008, 57, 371–374.

[4]. Bernard W. Ikua, Hisataka Tanaka, Fumio Obata, Satoshi Sakamoto. "Prediction of cutting forces and machining error in ball end milling of curved surfaces -I theoretical analysis". *Precision Engineering, 25(4): 266-273, 2001.*

[5]. S. M. Pandit and M. S. Shunmugan. "Signature of Machine Tool Errors on Surface Texture". *Annals of the CIRP*, PED-Vol. 45:63-74, 1990.

[6]. W.S. Lin, B.Y. Lee, C.L. Wu, Modeling the surface roughness and cutting force for turning, *Journal of Materials Processing Technology*. 108, 286–293, 2001.

[7]. O.B. Abouelatta, J. Madl, Surface roughness prediction based on cutting parameters and tool vibrations in turning operations, J. Mater. Process. Technol. 118, 269–277, 2001.

[8]. S. Fu, B. Muralikrishnan, and J. Raja, Engineering Surface Analysis with Different Wavelet Bases. Transactions of the ASME, 125, 844-852, 2003.

[9]. K.A. Risbood, U.S. Dixit, A.D. Sahasrabudhe, Prediction of surface roughness and dimensional deviation by measuring cutting forces and vibrations in turning process. Journal of Materials Processing Technology 132, 203–214, 2003.

[10].   G.B. Boothroyd and W. A. Knight. *Fundamentals of Machining and Machine Tools*, Marcel Dekker, Inc., New York, 1989.

[11].   K.F. Ehmann, S. G. Kapoor, R. E. DeVor, and I. Lazoglu. "Machine Process Modeling Review". *Journal of Manufacturing Science and Engineering*, 119:655-663, 1997

[12].   P. Albrecht. "Dynamics of the Metal Cutting Process". *J. of Engineering for Industry*. 87:429-441, 1965.

[13].   N.H. Hanna and S. A. Tobias. "A Theory of Nonlinear Regenerative Chatter". *J. of Engineering for Industry*, 96:247-253, 1974.

[14].   M.A. El Baradie. "Statistical Analysis of the Dynamic Cutting Coefficients and Machine Tool Stability". *J. of Engineering for Industry*, 115:205-214, 1993.

[15].   J. Peters and P. Vanherck. "Machine Tool Stability Tests and the Incremental Stiffness". *Annals of the CIRP*, 17:225-232, 1969.

[16].   S.M. Pandit, T.L. Subramanian, and S.M. Wu. "Modelling Machine Tool Chatter by Time Series". *J. of Engineering for Industry*, 97:211-215, 1975.

[17].   M.U. Jen and E. B. Magrab. "The Dynamic Interactive of the Cutting Process, Workpiece, and Lathe's Structure in Facing". *J. of Manufacturing Science and Engineering*, 118:348-357, 1998.

[18].   L. Kops, M. Gould, and M. Mizrach. " Improved Analysis of the Workpiece Accuracy in Turning Based on the Emerging Diameter". *J. of Engineering for Industry*, 115:253-257, 1993.

[19].   A.M. Shawky and M. A. Elbestawi. "An Enhanced Dynamic Model in Turning Including the Effects of Ploughing Force". *J. of Manufacturing Science and Engineering*, 119:10-20, 1997.

[20].   L.K. Daneshmend and H. A. Pak. "Model Reference Adaptive Control of Feed Force in Turning". *J. of Dynamic Systems, Measurements and Control*, 108:215-222, 1986

[21].   T.E. Bailey, D.M. Jenkins, A.D. Spence, and M.A. Elbestawi, "Integrated Modelling for Metal Removal Operations". *Proc. Of the ASME Dynamic Systems and Control Division*, 58:191-198, 1996.

[22].   Y. Tian, B. Shirinzadeh, D. Zhang. "A flexure-based mechanism and control methodology for ultra-precision turning operation". *Precision Engineering. 2009, 33, 160–166*

[23].   A.H. El-Sinawi. "Two-dimensional vibration suppression in turning using optimal control of the cutting tool". *Int. J. Machining and Machinability of Materials. 2008, Vol. 3, Nos. 1/2, 91-103.*

[24].   Hamed Moradi, M.R. Movahhedy, G. Reza Vossoughi. "Robust control strategy for suppression of regenerative chatter in turning". *Journal of Manufacturing Processes.* (2009) , 11, 55_65

[25].   S.N. Huang, K.K. Tan, Y.S. Wong, C.W. de Silva, H.L. Goh, W.W. Tan. "Tool wear detection and fault diagnosis based on cutting force Monitoring". *International Journal of Machine Tools & Manufacture*. 2007, 47, 444–451

[26].   Y. Zhu. "Estimation of an N-L-N Hammerstein-Wiener Model". *Automatica*. 2002, 38, 1607-1614.

[27].   A.H. El-Sinawi, A. H., and A. R. Kashani. "Improving surface roughness in turning using a Kalman estimator-based feed forward control of tool's position". *Journal of Materials Processing Technology*. 2005, 167, pp 54-61

[28]. M. Farina and L. Piroddi. "An iterative algorithm for simulation error based identification of polynomial input-output models using multi-step prediction". *International Journal of Control*, 83, Issue 7 July 2010 , 1442 – 1456.

[29]. L. Ljung. *System Identification: Theory for the User.* Prentice Hall; 2nd edition, 1999

[30]. A.H. El-Sinawi. "Vibration attenuation of a flexible beam mounted on a rotating compliant hub". Journal of Systems and Control Engineering, Part I, April, 2004, *218,* pp 121-135.

[31]. W. Gawronsky. *Advanced Structural Dynamics and Active Control of Structures*. Springer-Verlag, 2004.
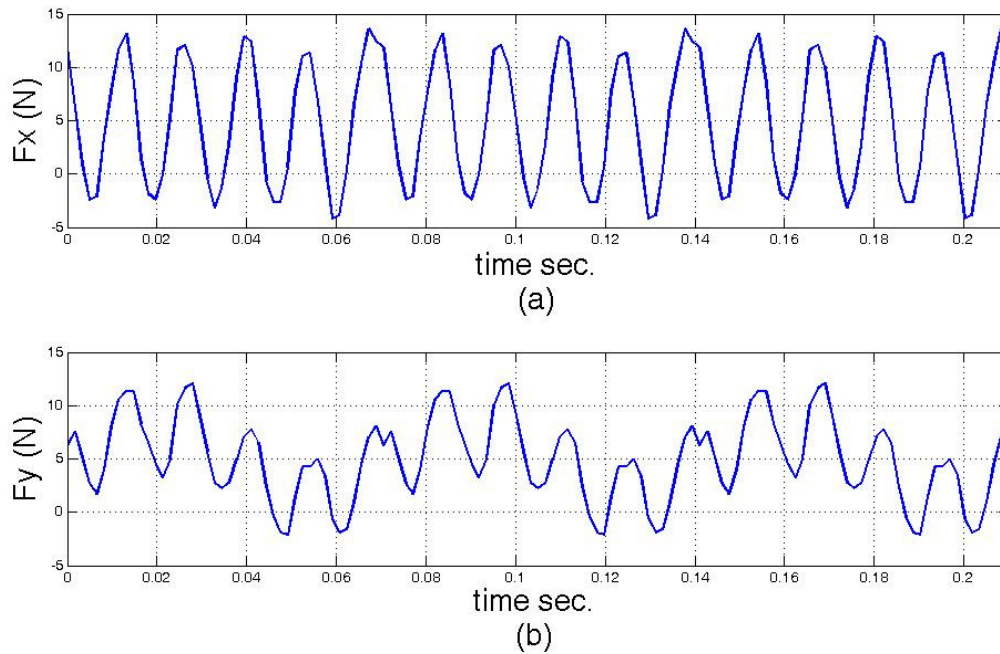
FIGURE 1: Sample of experimental dynamic cutting forces in (a) radial and (b) tangential directions.
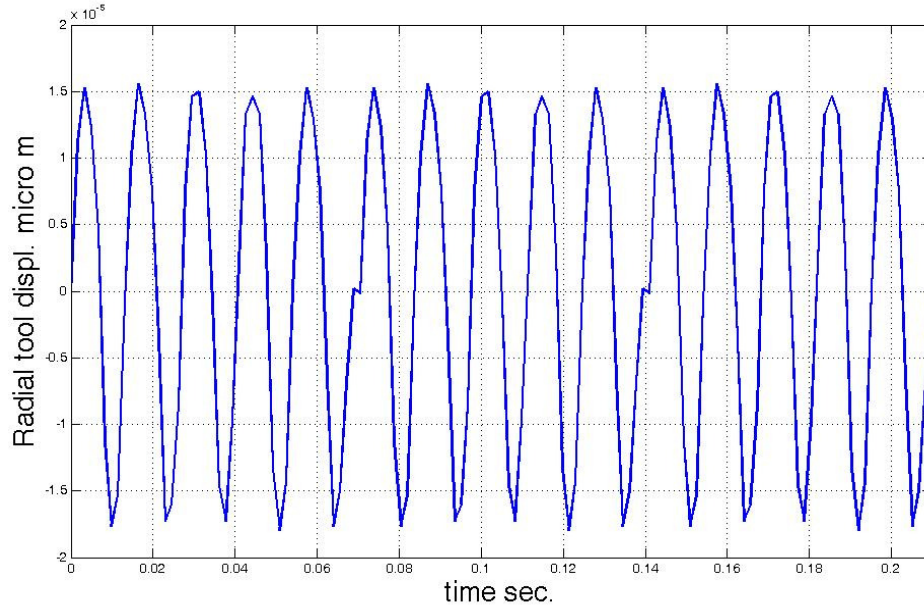
FIGURE 2: Tool displacement in the radial direction measurements during orthogonal cutting
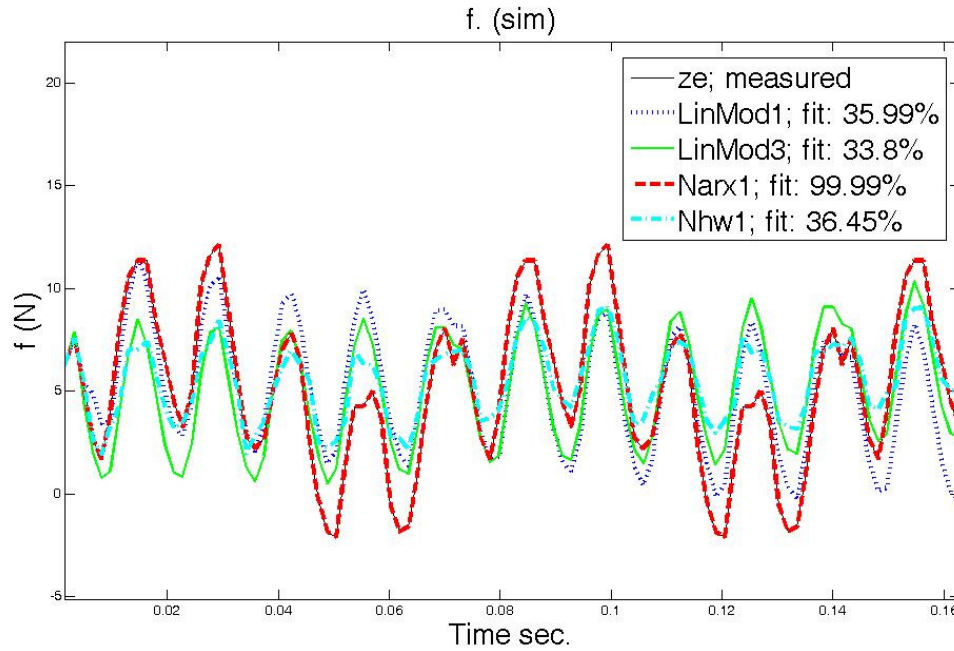
FIGURE 3: Nonlinear models constructed from experimental results
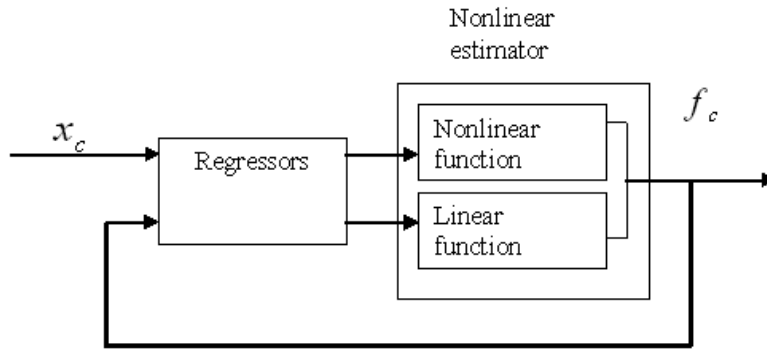
FIGURE 4: Nonlinear ARX model structure
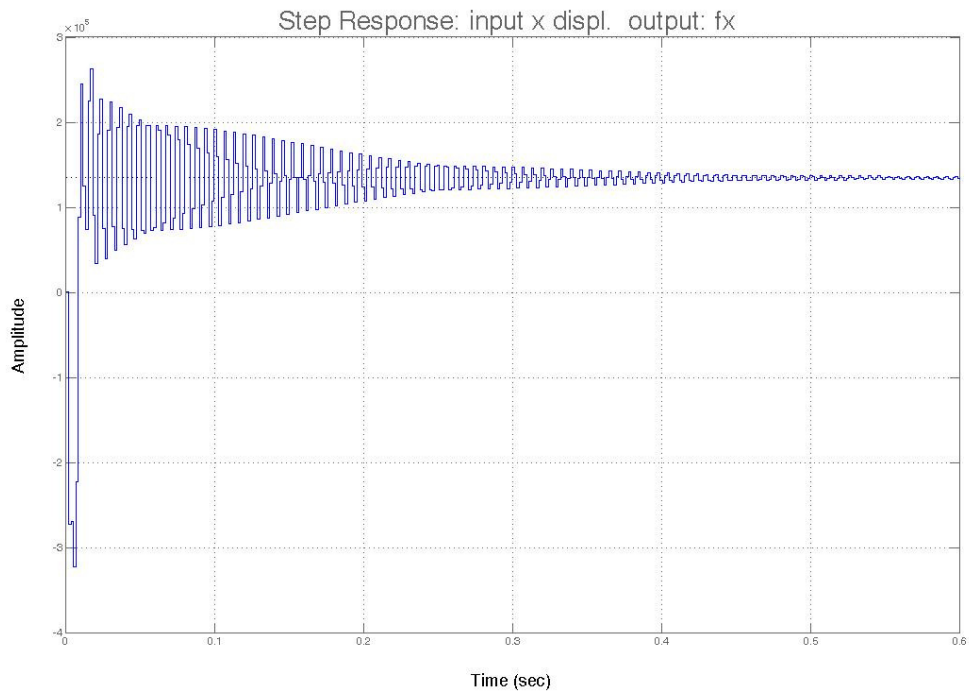
FIGURE 5: Step response of the radial force model f_x
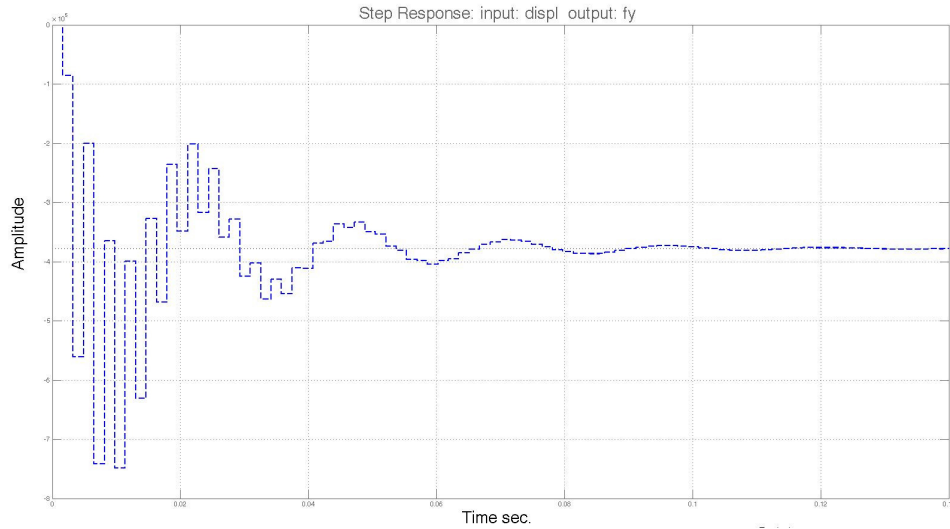
**FIGURE 6**: Step response of the tangential force model f_y
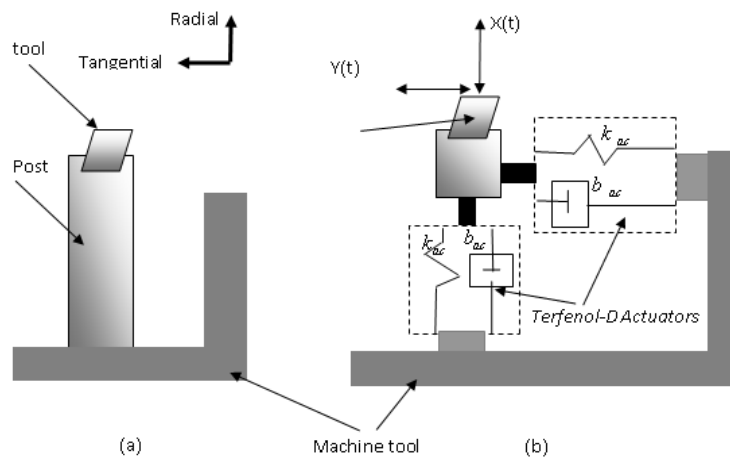
FIGURE 7: (a) Conventional machine tool, (b) machine tool retrofitted with two actuators transducer for cutter manipulation. *v(t)* measurements noise.
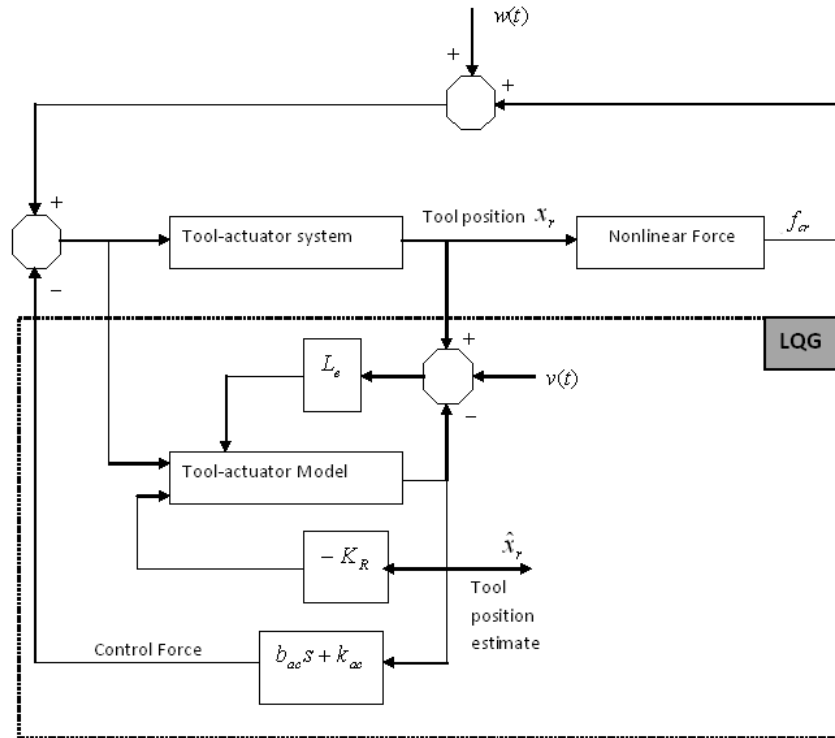
FIGURE 8: Controller implementation in the radial direction (i.e., x-direction)
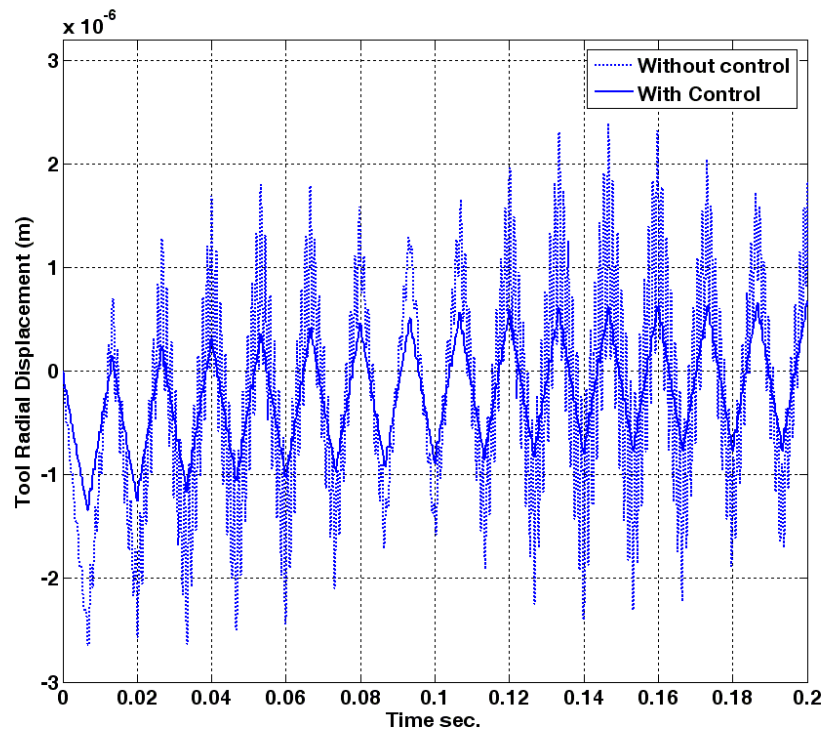
**FIGURE 9**: tool dynamic displacement in the radial direction
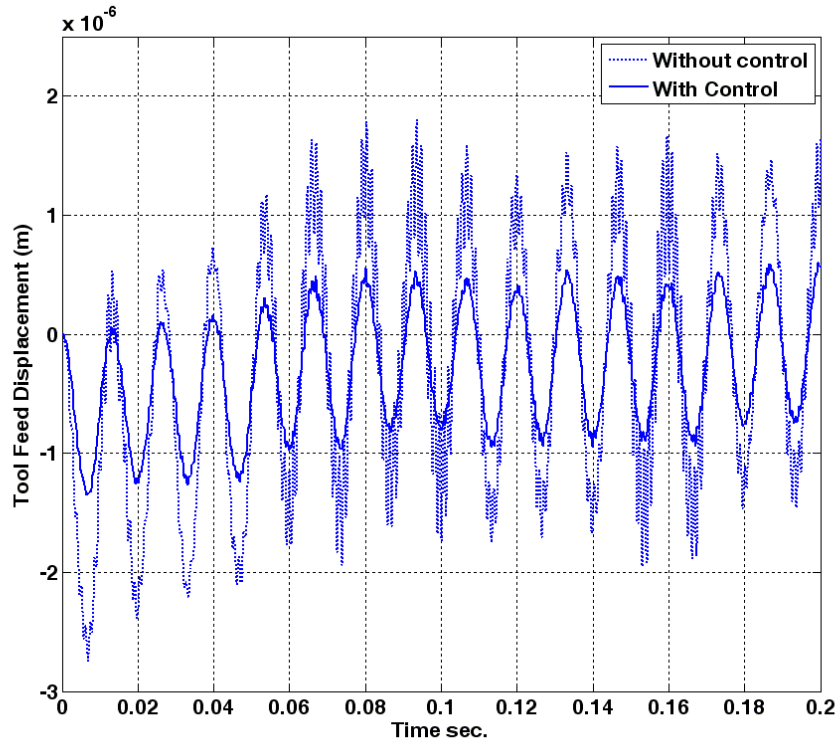
**FIGURE 10**: tool dynamic displacement in the tangential direction
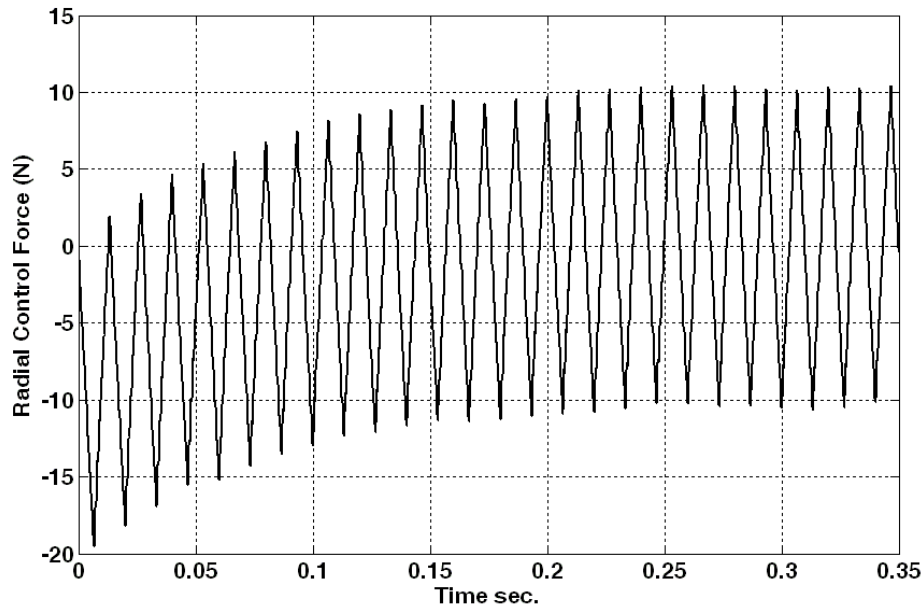
FIGURE 11: Control force in radial direction

A.H. El-Sinawi
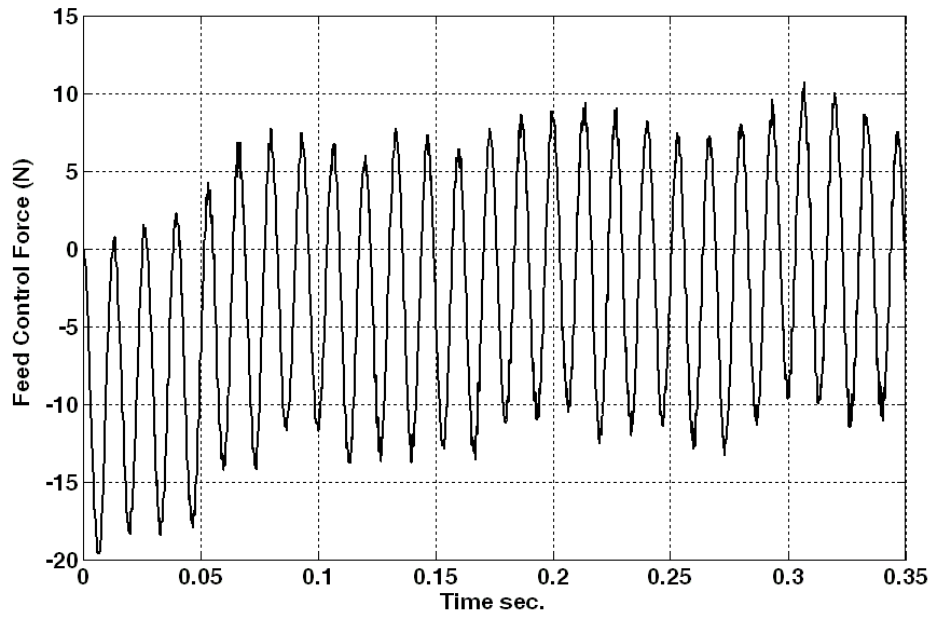
FIGURE 12: Control force in the feed direction

Appendix A: Linearization of a Nonlinear system [29]

Common use of time-varying linear systems is related to linearization of nonlinear systems around a certain "nominal" trajectory. Therefore, for a nonlinear system described by

$$x(t+1) = f((x(t),u(t)) + r(x(t),u(t))w(t)$$
$$y(t) = h(x(t)) + m(x(t),u(t))v(t)$$

a.1

Assuming that the disturbance terms $w(t)$ and $v(t)$ are white and small, with the nominal and disturbance-free ($w(t) \equiv 0$, $v(t) \equiv 0$) behavior of the system corresponds to an input sequence $u^*(t)$ and corresponding trajectory $x^*(t)$. Neglecting nonlinear terms, the differences,

$$\Delta x(t) = x(t) - x^*(t)$$
$$\Delta y(t) = y(t) - h(x^*(t))$$
$$\Delta u(t) = u(t) - u^*(t)$$

Are then subjected to

$$\Delta x(t+1) = F(t)\Delta x(t) + G(t)\Delta u(t) + \overline{w}(t)$$
$$\Delta y(t) = H(t)\Delta x(t) + \overline{v}(t)$$

a.2

Such that,

$$F(t) = \left.\frac{\partial}{\partial x}f(x,u)\right|_{x^*(t),u^*(t)} \quad, \quad G(t) = \left.\frac{\partial}{\partial u}f(x,u)\right|_{x^*(t),u^*(t)} \quad, \quad H(t) = \left.\frac{\partial}{\partial x}h(x)\right|_{x^*(t)}$$

In view of the assumption of small disturbances, the cross terms with disturbance. The terms $\overline{w}(t)$ and $\overline{v}(t)$ in Eq. a.2 above are white disturbances with the following covariance properties:

$$R_1(t) = E\,\overline{w}(t)\overline{w}^T(t) = r(x^*(t),u^*(t))E\,w(t)w^T(t)\,r^T(x^*(t),u^*(t))$$
$$R_2(t) = E\,\overline{v}(t)\overline{v}^T(t) = m(x^*(t),u^*(t))E\,v(t)v^T(t)m^T(x^*(t),u^*(t))$$
$$R_{12}(t) = r(x^*(t),u^*(t))E\,w(t)v^T(t)m^T(x^*(t),u^*(t))$$

a.3

The model is now linear in the vicinity of nominal trajectory.